

UC San Diego

UC San Diego Previously Published Works

Title

Global emissions of refrigerants HCFC-22 and HFC-134a: Unforeseen seasonal contributions

Permalink

<https://escholarship.org/uc/item/6fb3938z>

Journal

Proceedings of the National Academy of Sciences of the United States of America, 111(49)

ISSN

0027-8424

Authors

Xiang, Bin
Patra, Prabir K
Montzka, Stephen A
et al.

Publication Date

2014-12-09

DOI

10.1073/pnas.1417372111

Peer reviewed

Global emissions of refrigerants HCFC-22 and HFC-134a: Unforeseen seasonal contributions

Bin Xiang^{a,1}, Prabir K. Patra^b, Stephen A. Montzka^c, Scot M. Miller^a, James W. Elkins^c, Fred L. Moore^{c,d}, Elliot L. Atlas^e, Ben R. Miller^{c,d}, Ray F. Weiss^f, Ronald G. Prinn^g, and Steven C. Wofsy^a

^aSchool of Engineering and Applied Sciences, Harvard University, Cambridge, MA 02138; ^bDepartment of Environmental Geochemical Cycle Research, Japan Agency for Marine–Earth Science and Technology, Yokohama 236 0001, Japan; ^cNational Oceanic and Atmospheric Administration Earth System Research Laboratory, Global Monitoring Division Halocarbon and other Trace Gases Group, Boulder, CO 80305; ^dCooperative Institute for Research in Environmental Sciences, University of Colorado, Boulder, CO 80309; ^eDepartment of Atmospheric Sciences, Rosenstiel School of Marine & Atmospheric Science, University of Miami, Miami, FL 33149; ^fGeosciences Research Division, Scripps Institution of Oceanography, University of California at San Diego, La Jolla, CA 92093; and ^gDepartment of Earth, Atmospheric, and Planetary Sciences, Massachusetts Institute of Technology, Cambridge, MA 02139

Edited by A. R. Ravishankara, Colorado State University, Fort Collins, CO, and approved October 22, 2014 (received for review September 11, 2014)

HCFC-22 (CHClF₂) and HFC-134a (CH₂FCF₃) are two major gases currently used worldwide in domestic and commercial refrigeration and air conditioning. HCFC-22 contributes to stratospheric ozone depletion, and both species are potent greenhouse gases. In this work, we study in situ observations of HCFC-22 and HFC-134a taken from research aircraft over the Pacific Ocean in a 3-y span [Hlaper-Pole-to-Pole Observations (HIPPO) 2009–2011] and combine these data with long-term ground observations from global surface sites [National Oceanic and Atmospheric Administration (NOAA) and Advanced Global Atmospheric Gases Experiment (AGAGE) networks]. We find the global annual emissions of HCFC-22 and HFC-134a have increased substantially over the past two decades. Emissions of HFC-134a are consistently higher compared with the United Nations Framework Convention on Climate Change (UNFCCC) inventory since 2000, by 60% more in recent years (2009–2012). Apart from these decadal emission constraints, we also quantify recent seasonal emission patterns showing that summertime emissions of HCFC-22 and HFC-134a are two to three times higher than wintertime emissions. This unforeseen large seasonal variation indicates that unaccounted mechanisms controlling refrigerant gas emissions are missing in the existing inventory estimates. Possible mechanisms enhancing refrigerant losses in summer are (i) higher vapor pressure in the sealed compartment of the system at summer high temperatures and (ii) more frequent use and service of refrigerators and air conditioners in summer months. Our results suggest that engineering (e.g., better temperature/vibration-resistant system sealing and new system design of more compact/efficient components) and regulatory (e.g., reinforcing system service regulations) steps to improve containment of these gases from working devices could effectively reduce their release to the atmosphere.

HCFC-22 | HFC-134a | refrigerants | global emissions | emission seasonality

CFC-12 (dichlorodifluoromethane, CCl₂F₂), HCFC-22 (chlorodifluoromethane, CHClF₂), and HFC-134a (1,1,1,2-tetrafluoroethane, CH₂FCF₃) are major coolants used in domestic and commercial refrigeration and air conditioning. Because of their ubiquitous use, these three gases are the most abundant of the chlorofluorocarbon (CFC), the hydrochlorofluorocarbon (HCFC), and the hydrofluorocarbon (HFC) species categories, respectively, in Earth's atmosphere. Due to their role in depleting stratospheric ozone (1), production and/or consumption of all CFCs were scheduled to be phased out gradually by the Montreal Protocol, first from developed countries by 1996, followed by developing countries by 2010. HCFC-22 has an ozone-depleting potential (ODP) about 20 times less than that of CFC-12 and so partly became an interim replacement for CFC-12 beginning in the late 1980s (HCFC-22 has had other significant uses such as propellants and foam blowing beginning in the early 1970s). Production and emissions of HFC-134a began slightly later, in the early 1990s, as a preferred component of

motor vehicle air conditioning systems to replace CFC-12. Both HCFC-22 and HFC-134a are potent greenhouse gases, with global warming potentials (GWPs) of 1,760 and 1,300 on a 100-y time scale (2). The production of HFC-134a is anticipated to continue, and its emissions will very likely increase, until transition is made to refrigerants with low ODPs and GWPs (3).

Country-based annual consumption and production magnitudes for the HCFCs and emission data for HFC-134a have been collected since the 1990s, by the United Nations Environment Program (UNEP) and the United Nations Framework Convention on Climate Change (UNFCCC), respectively. National-scale emissions are difficult to accurately quantify from these consumption and production data (4). First, there is usually a delay time from production of these gases to actual atmospheric release. This delay, known as the bank effect, ranges from near zero to decades, depending on how the chemicals are used (5). Second, production and emission data from reporting countries are neither audited nor independently verified under the Montreal and the Kyoto Protocols (6, 7). Finally, HFC emissions reported by the UNFCCC do not represent global totals because they do not currently include emissions from developing countries.

In contrast to these “bottom-up” estimates, a number of other studies have used observations of atmospheric concentrations, atmospheric transport models, and inversion methods to derive

Significance

HCFC-22 (CHClF₂) and HFC-134a (CH₂FCF₃) are two major gases currently used worldwide in domestic and commercial refrigeration and air conditioning. HCFC-22 contributes to stratospheric ozone depletion, and both species are potent greenhouse gases. We find pronounced seasonal variations of global emissions for these two major refrigerants, with summer emissions two to three times higher than in winter. Thus results suggest that global emissions of these potent greenhouse gases might be mitigated by improved design and engineering of refrigeration systems and/or by reinforcing system service regulations.

Author contributions: B.X. and S.C.W. designed research; B.X., P.K.P., S.A.M., J.W.E., F.L.M., E.L.A., B.R.M., R.F.W., R.G.P., and S.C.W. performed research; B.X. contributed new reagents/analytic tools; B.X. analyzed data; B.X. and S.M.M. wrote the paper; P.K.P. ran the ACTM model; and S.A.M., J.W.E., F.L.M., E.L.A., B.R.M., R.F.W., and R.G.P. collected the data.

The authors declare no conflict of interest.

This article is a PNAS Direct Submission.

Data deposition: HIPPO Data are archived at the Carbon Dioxide Information Analysis Center (CDIAC), Oak Ridge National Laboratory (ORNL), hippo.ornl.gov. AGAGE data are archived at the CDIAC, ORNL, US Department of Energy (DOE), cdiac.ornl.gov/ndps/alegale.html. NOAA data are archived by the NOAA ESRL GMD HATS group, www.esrl.noaa.gov/gmd/hats/data.html.

¹To whom correspondence should be addressed. Email: bxiang@seas.harvard.edu.

This article contains supporting information online at www.pnas.org/lookup/suppl/doi:10.1073/pnas.1417372111/-DCSupplemental.

regional-scale emissions. These so-called “top–down” studies can improve the spatial and temporal distribution of bottom–up inventories and provide insights on the associated emission mechanisms that may be used as information for climate change mitigation. Most recent top–down studies of HCFC-22 and HFC-134a indicate lower US emissions and higher emissions in Europe, Australia, and Asia than in the existing inventories (8–11).

The seasonal variation in the emissions has been generally overlooked in the past. Refrigerant leakage studies suggest neither the gradual leaks (i.e., regular emissions) nor the immediate release (i.e., break of the air conditioning system) have significant seasonal dependences (12, 13). In contrast, a few regional atmospheric studies suggest that emissions of HCFC-22 and HFC-134a may be seasonal due to weather-dependent patterns in refrigerator and air conditioner use (14–19). This uncertainty in seasonality indicates incomplete knowledge of the underlying mechanisms that lead to atmospheric release. Effective emission control strategies depend on understanding the processes that cause these refrigerant emissions.

In this study, we quantify the seasonality of emissions and derive total global emission budgets for HCFC-22 and HFC-134a, using top–down approaches. The current study advances previous top–down efforts by using a full tropospheric (i.e., latitudinal and altitudinal) observation dataset over the Pacific Ocean from the HIAPER-Pole-to-Pole Observation (HIPPO) aircraft campaign to complement ground-based measurements, to better constrain global spatiotemporal emission patterns for HCFC-22 and HFC-134a during 2009–2011. A 3D atmospheric chemistry-transport model (ACTM) (*SI Materials and Methods*) with independently validated chemistry and transport is used for model/data comparison and emission optimization (20).

Data Overview and Top–Down Approach

The global atmospheric observation data used in this study come from both long-term remote surface observation sites and aircraft campaigns. The ground measurements were made by the National Oceanic and Atmospheric Administration Earth System Research Laboratory (NOAA ESRL) (21, 22) and by the Advanced Global Atmospheric Gases Experiment (AGAGE) (23, 24) networks from the late 1970s to the present. Results from earlier years are provided from firn air measurements (25) or the analysis of archived air samples (beginning in the late 1970s) and later from an ongoing collection of samples at up to 21 (present) surface sites over the globe for HCFC-22 and HFC-134a (locations in Fig. S1).

In addition to these ground sites, the HIAPER-Pole-to-Pole Observation of Carbon Cycle and Greenhouse Gases Study (HIPPO) provides aircraft observations of atmospheric composition over the Pacific Ocean, in different seasons between 2009 and 2011 (HIPPO-1, January 2009; HIPPO-2, October/November 2009; HIPPO-3, March/April 2010; HIPPO-4, June/July 2011; and HIPPO-5, August/September 2011) (26). Observations span from 87° North to 67° South latitude with vertical profiles approximately every 2.2° in latitude. These profiles span from near the surface (150 m) to a maximum of 15 km altitude (flight tracks in Fig. 1 and Fig. S1). A total of 2,370 flask and 3,663 gas chromatography (GC) sampling data for HCFC-22 and 2,485 flasks and 3,344 GC samples for HFC-134a were collected during all five HIPPO missions (*SI Materials and Methods*).

Each HIPPO mission lasted about 1 mo with near pole-to-pole coverage. The good agreement between results from HIPPO (at low altitudes) and those from ground sites (monthly averages) indicates the global representation of the HIPPO gas composition measurements in both temporal changes and latitudinal gradients (Fig. S2). In addition, HIPPO measurements provide the opportunity to study atmospheric transport and chemistry mechanisms in the upper troposphere. Fig. 1 shows typical HIPPO observations during March 2010 and corresponding model simulations for

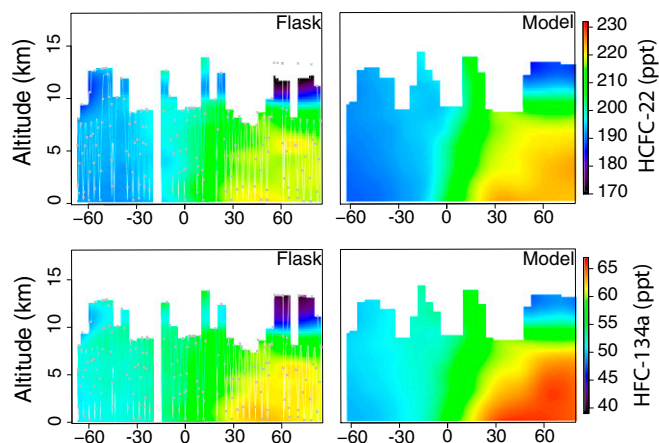


Fig. 1. Curtain plots of observed HCFC-22 (Top Row) and HFC-134a (Bottom Row) mixing ratios during HIPPO-3 northbound flights (Left Column), and simulated by ACTM (Right Column, using scaled United Nations inventories). HIPPO flight track and NWAAS flask sampling locations are indicated as white lines and cross symbols separately.

both refrigerant species. HIPPO observations reveal detailed height–latitude atmospheric distribution features. These features include evidence for major emissions in the northern hemisphere, transported by vertical motions and zonal and meridional winds. The data show sharp horizontal concentration gradients at air mass boundaries, with relatively weak vertical gradients, notably in the tropics.

In this study, we optimize existing HCFC-22 and HFC-134a emissions estimates such that modeled atmospheric mixing ratios match atmospheric observations, known as a top–down approach. As a first step, we use the surface observations (i.e., all available sites from NOAA and AGAGE) to examine historical changes in emissions. To accomplish this, we estimate a single global scaling factor in each year for the existing or converted emission inventories [i.e., Global Emission Inventory Activity (GEIA), UNEP, and UNFCCC] (Fig. S3 and *SI Materials and Methods*) for each species between the 1980s and 2012, to best match the corresponding observed atmospheric mixing ratios and growth rates at all AGAGE and NOAA sites (Fig. S4 and *SI Materials and Methods*). We then conduct separate inversions for each of the four HIPPO missions over 53 land regions (Fig. S5 and *SI Materials and Methods*). Long-term observations from NOAA and AGAGE surface sites ensure accurate annual emission trends for the recent 3-y HIPPO sampling period, a prerequisite for our seasonal emission inversions. Surface observations are also used for independent validations of our derived emissions. Meanwhile, HIPPO provides data-dense upper tropospheric snapshots that are ideal for estimating the spatial and seasonal distributions of emissions.

Emission Changes over Time in Response to the Montreal Protocol

Emissions of HFC-134a and CFC-12 changed quickly after implementation of the Montreal Protocol (Fig. 2). In particular, we find that emissions of CFC-12 dropped shortly after the initial signing of the Montreal Protocol in 1987 (about 50% decrease over the following 5 y). Furthermore, emissions of both CFC-12 and HCFC-22 showed step changes in 2005 (15 Gg/y reduction and 35 Gg/y increase, respectively, in response to the corresponding UNEP production changes; ozone.unep.org/new_site/en/ozone_data_tools_access.php), a year when developing countries were first required to make reductions (50%) of CFC-12 production by the Montreal Protocol. However, we do not find abrupt emission changes in either species in 1996 or 2010, the required CFC-12 phase-out deadlines from developed and developing

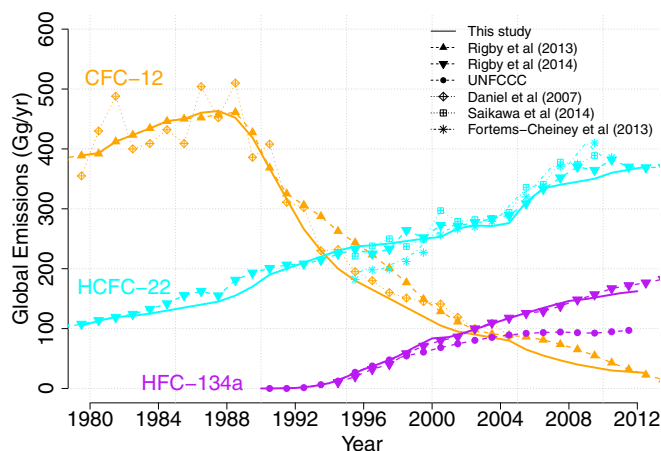


Fig. 2. Optimized global total emissions of HCFC-22, HFC-134a, and CFC-12 based on global surface monitoring site observations and ACTM simulations. Our results are compared with earlier studies derived from similar observations (11, 18, 34, 35) or inventories (UNFCCC) (4).

countries, respectively. These results are consistent with the gradually declining CFCs production data from UNEP. The results also suggest that countries phased out production well ahead of the mandated deadline; bank storage likely dominated CFC-12 emissions in more recent years (27).

Emissions of HFC-134a have increased consistently and indeed accelerated, from 1990 through 2012. Our emission estimates disagree with and become higher than the magnitudes reported to UNFCCC after year 2000 (by more than 60% in 2009–2012). Because most non-Annex I parties (i.e., developing countries) in UNFCCC are not obliged to report their emissions, this discrepancy is likely due to the unreported contribution from developing countries. This emission discrepancy could also be partly due to inaccuracies in reporting from Annex-I countries (i.e., developed countries), which are predominantly inventory based (28).

Seasonal Trends in Emissions

Seasonal Discrepancies Between the Model and Observations. We observe persistent seasonal variations in HCFC-22 and HFC-134a atmospheric concentrations measured at surface sites. A number of factors could account for the observed seasonal cycles: seasonality in the emissions, changes in atmospheric oxidation (via the OH fields), and seasonal changes in atmospheric transport (e.g., stratosphere–troposphere exchange, boundary layer trapping, interhemispheric exchange, large-scale horizontal transport, and mixing in the upper troposphere). The relative contribution of each process varies globally.

The atmospheric model simulates a seasonal cycle at most northern hemisphere ground sites that is very different from what is observed. The surface station at Barrow (BRW), Alaska, provides a useful case in point (Fig. 3A). Observations at BRW show a broad winter maximum and summer minimum. Model seasonality [using the aseasonal GEIA and the United Nations (UN)-derived emission inventories], in contrast, has a larger amplitude and is phase shifted compared with the observations. The seasonality in the model is dominated by the increased scavenging through the OH radical reaction and seasonality in the transport. However, these two factors alone cannot explain the seasonal features in the observations. Model-simulated methyl chloroform (CH_3CCl_3) and sulfur hexafluoride (SF_6) match their observed seasonal cycles fairly well at BRW ($r = 0.98$ and 0.86 , respectively).

The model/data mismatch for the refrigerants also applies for other northern hemisphere (NH) sites, such as Mace Head (MHD) (Ireland) shown in Fig. 3A and Trinidad Head (THD) (California), Mauna Loa (MLO) (Hawaii), and Ragged Point (RPB) (Barbados)

shown in Fig. S64. Meanwhile in the southern hemisphere where emissions are small [e.g., American Samoa (SMO), Cape Grim (CGO) (Australia), and South Pole (SPO)], both target gases show good model/data agreement (Fig. S64). To this end, we believe that emissions are the largest cause of the discrepancies between observed and simulated seasonal cycles of refrigerants.

Large seasonal model–data mixing ratio differences are also apparent in HIPPO (Fig. 4). The model simulates that the NH latitudinal gradients of HCFC-22 and HFC-134a mixing ratios for HIPPO-3 (March 2010) are slightly larger than the corresponding observations. This result suggests that during the boreal winter, the NH mid- to high-latitude emissions are lower than the annual average of the emissions. In contrast to winter and springtime, model simulations of HCFC-22 and HFC-134a during summertime (e.g., HIPPO-5 in August 2011) are consistently lower than observations at all NH latitudes. This result indicates that the northern regional summertime emissions should be higher than the annual average.

Emission Seasonal Cycle Estimated from HIPPO Inversions. In this section, we use the atmospheric observations to quantify global

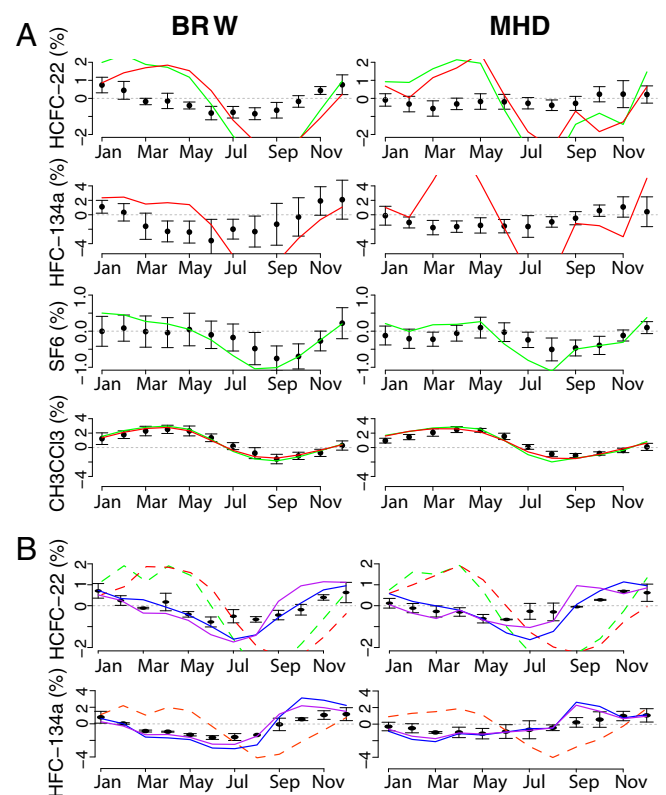


Fig. 3. (A) Observed and simulated seasonal cycles of HCFC-22, HFC-134a, SF_6 , and CH_3CCl_3 mixing ratios averaged over the period of 1996–2012, at two selected surface sites, namely, Barrow, Alaska (71.2°N , 156.6°W , NOAA) and Mace Head, Ireland (53.3°N , 9.9°W , AGAGE). See Fig. S6 for more sites. Both observations (symbols) and model simulations (lines) are subtracted by their corresponding 12-mo moving averages. The detrended signals are further normalized by the corresponding annual mean mixing ratio (y axis presented in percentage). The error bars show 1 SD of the interannual variability at each month. ACTM simulations use the scaled United Nations inventories (red; UNEP derived for HCFC-22 and CH_3CCl_3 and UNFCCC for HFC-134a) and other available inventories (green; GEIA for HCFC-22, EDGAR4.2 for SF_6 , and TransCom- CH_4 for CH_3CCl_3); emissions from these inventories are constant throughout the year. (B) Same as A for HCFC-22 and HFC-134a but over the HIPPO period of 2009–2011. In addition, ACTM simulations use two more emission scenarios: scaled UN inventory with seasonal adjustments (blue) and scaled UN inventory with both seasonal and spatial adjustments (purple).

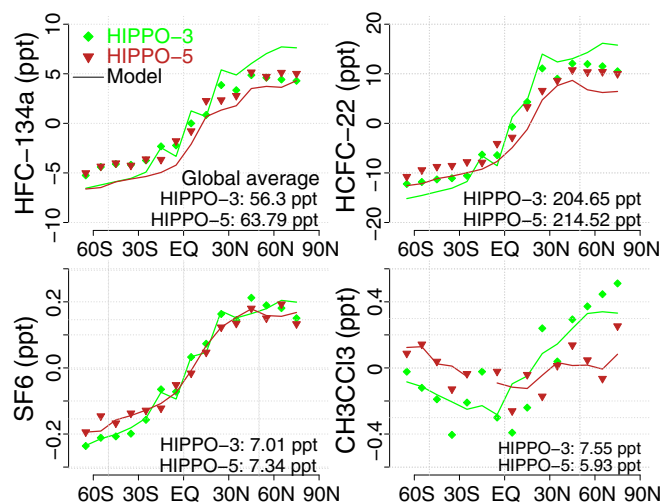


Fig. 4. Tropospheric mean mixing ratios of HCFC-22, HFC-134a, SF₆, and CH₃CCl₃ from HIPPO mission 3 in winter and mission 5 in summer (symbols; weighted by pressure for every 10° latitudinal bin) and corresponding forward ACTM simulations using scaled inventory emissions (lines). Both observation and simulation data have been adjusted by subtracting with the global average mixing ratios from corresponding HIPPO observations (indicated in each plot). See Fig. S8 for the complete five HIPPO missions.

emissions by season. We conduct inversions over the time between HIPPO deployments, for both HFC-134a and HCFC-22. In short, we initiated monthly pulse emissions from 53 land regions between two adjacent HIPPO missions and tagged the enhanced signals in the ACTM model to form the sensitivity matrices. Then we used a Bayesian approach and set the model–data mismatch covariance matrix to include the measurement uncertainty and the model transport and chemistry errors (inferred from the HIPPO SF₆ and CH₃CCl₃ tracers, respectively). A total of 10,000 inversion realizations are performed in a bootstrap framework for

uncertainty estimation (*SI Materials and Methods*). Table 1 summarizes the resulting seasonal emissions of both species for the globe and two hemispheres, based on all four HIPPO inversions. Fig. 5 shows the latitudinal binned emissions of HFC-134a and HCFC-22 that resulted from the boreal winter period inversion (HIPPO-3) and the boreal summer period inversion (HIPPO-5), separately. Detailed global emission maps derived from inversions and their differences compared with the inventories are shown in Fig. S7.

Our most important finding from HIPPO inversions is that NH summertime emissions are triple the winter emissions for HFC-134a (3.04 [1.28, 5.18]) and more than double for HCFC-22 (2.31 [1.34, 6.27]), a seasonality much larger than estimated in most previous studies and emission inventories (ratios are from paired HIPPO-5 and -3 inversion results, using the same uncertainty estimations in each of the 10,000 realizations; data are presented as median values and the 16th and the 84th percentiles for the confidence interval). This result implies that a temperature- or use-dependent mechanism must control the majority of emissions, a result that contrasts with the assumptions made by existing inventories. A better understanding of the underlying processes could help effectively target and reduce the summertime peak emissions.

Validation Using Surface Observations. We validate the seasonality in emissions derived from HIPPO inversion, by adding this feature to emissions and using them in a forward model simulation to compare with observations at eight global surface sites during 2009–2011 (*SI Materials and Methods*). These simulations show much better agreement with observations compared with the aseasonal emissions model (Fig. 3B and Fig. S6B), particularly at the NH mid- and high-latitudes closest to the regions with highest HFC-134a and HCFC-22 emissions. For example, at BRW, the emission rates incorporating HIPPO-derived seasonality now simulate the correct amplitude and timing of the HFC-134a seasonal cycle, reducing the model–data disagreement on a monthly timescale by 45% compared with the seasonally invariable inventory (rmse from 2.22 to 1.23). The corresponding improvements

Table 1. Recent global emissions of HFC-134a and HCFC-22 based on inventories and inversion results from this study

Mission	Start time	Inversion season,* boreal	r^2		Global emissions, Gg/mo	NH emissions, Gg/mo	SH emissions, Gg/mo
			Prior	Posterior			
HFC-134a inversion							
HIPPO-1	January 2009						
HIPPO-2	October 2009	Late winter–early autumn	0.58	0.65	8.51 [†] [8.38, 8.90]	7.26 [5.41, 8.01]	1.23 [0.37, 3.49]
HIPPO-3	March 2010	Late autumn–winter	0.63	0.77	3.44 [2.25, 6.27]	3.26 [0.61, 6.12]	0.23 [0.12, 1.63]
HIPPO-4	June 2011	Four seasons	0.84	0.86	11.42 [10.76, 11.51]	9.08 [8.53, 9.59]	2.21 [1.12, 2.96]
HIPPO-5	August 2011	Summer	0.86	0.88	11.06 [8.94, 16.35]	9.64 [8.49, 10.85]	1.42 [0.41, 5.42]
HFC-134a inventory							
UNFCCC	2009–2011	Seasonal invariant			7.89 [§]	7.65	0.24
HCFC-22 inversion							
HIPPO-1	January 2009						
HIPPO-2	October 2009	Late winter–early autumn	0.68	0.72	24.75 [†] [24.16, 26.63]	22.65 [18.61, 25.06]	1.70 [1.16, 6.21]
HIPPO-3	March 2010	Late autumn–winter	0.65	0.75	12.47 [6.59, 21.51]	12.47 [5.14, 21.05]	0.30 [0, 1.69]
HIPPO-4	June 2011	Four seasons	0.83	0.85	28.50 [28.16, 28.85]	27.30 [27.22, 27.39]	1.19 [0.87, 1.55]
HIPPO-5	August 2011	Summer	0.79	0.80	30.74 [30.00, 33.78]	28.83 [28.10, 32.22]	1.90 [1.56, 1.91]
HCFC-22 inventory							
UNEP derived	2009–2011	Seasonal invariant			29.88 [§]	27.98	1.89

*Inversion time period is between this and previous HIPPO mission. See *SI Materials and Methods* for the detailed inversion setup.

[†]Statistical measure of model–data mixing ratio fit before and after the inversion.

[‡]Data are the median of 10,000 inversion sensitivity run results where the error covariance matrices for the mixing ratio data and for the prior emissions are varied. Emissions results from these inversions are not normally distributed. The 16th and 84th percentiles (equivalent to 1 SD in Gaussian distribution) are in brackets. See *SI Materials and Methods* for details.

[§]Averaged global total between 2009 and 2011. The emission interannual variability during this period (+3% y⁻¹ from UNFCCC and +2% y⁻¹ from UNEP derived) is well accounted for under the prior uncertainty estimates (>6% for HFC-134a and >8% for HCFC-22) in our inversion.

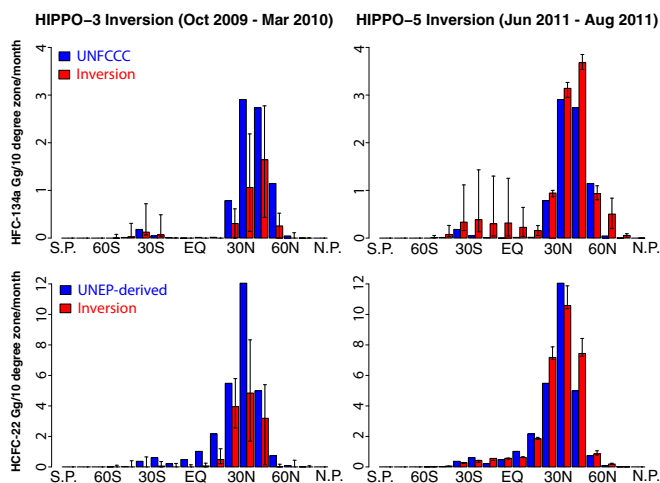


Fig. 5. Latitudinal emissions of HFC-134a (*Top*) and HCFC-22 (*Bottom*) from inventories (blue) and derived from inversions of HIPPO data (red) for boreal winter (*Left*) and summer (*Right*). Results are median values from 10,000 inversion sensitivity runs; error bars are the 16th and 84th percentiles. The prior emissions (i.e., emission inventories) are much farther from the best estimate of the fluxes in HIPPO-3 inversion than in HIPPO-5 and the emission rates are smaller, causing larger uncertainties in the final estimates.

for all five NH ground sites (BRW, MHD, THD, MLO, and RPB) are on average $43 \pm 24\%$ for HFC-134a and $61 \pm 15\%$ for HCFC-22. Although our sensitivity test of the inverse model-derived emission seasonality (*SI Materials and Methods*) has a large confidence interval, the validation against surface sites in this section gives us added confidence that a summer-to-winter ratio of between 2 and 3 is most realistic (Fig. 3*B* and Fig. S6*B*).

Possible Mechanisms for Refrigerant Emission Seasonality. Refrigerators and air conditioners (AC) may leak more in summer than in winter due to higher internal system pressure and more frequent use, both associated with higher ambient temperature in summer.

Even when not in use, both HFC-134a and HCFC-22 in sealed refrigeration systems have higher vapor pressures in summer than in winter, by factors between 2 and 3. As a reference, the saturation vapor pressure is 293.0 kPa at 273 K and 770.8 kPa at 303 K for HFC-134a and 498.0 kPa at 273 K and 1192.0 kPa at 303 K for HCFC-22 (Technical Information, DuPont Refrigerants). The high vapor pressures in summer, roughly 8–12 times atmospheric pressure, may promote leakage past seals in the refrigeration systems. In use, both refrigerants have much higher pressures in the compressor line compared with when not in use (e.g., ~ 4 times for HFC-134a systems) (12). This even higher vapor pressure during operation, combined with more frequent use of cooling devices in summer, could lead to enhanced leak rates in summer compared with winter. The association of leak rates with higher vapor pressure in summer seems consistent with the slightly less emission seasonality of HCFC-22 (2.31, summer to winter), used mainly in stationary applications, compared with that of HFC-134a (3.03), used mainly in mobile systems exposed to more extreme environmental temperatures.

In addition to the above-described “normal leaks” due to the poor sealing, there are episodic and service leaks of HFC-134a, associated with mobile air conditioner (MAC) system failures that mostly occur during the summer months. Episodic leaks vent all of the coolant in a system, due to internal (e.g., mechanical

and heat stress during use and subsequent deterioration of the seals) and external factors (e.g., car accidents and stone impacts), generally followed by service repairs (13). Two surveys dating and counting the AC-related motor vehicle workshop visits were conducted independently in Germany and California (29, 30). Both showed that the five summer months (May–September) account for $\sim 70\%$ of the annual total AC service visits, implying more frequent MAC defects during the warmer time of the year. Service and disposal procedures for the MAC system include leak test, charging, refill, and recovery; leaks during these procedures can be large if the service staff or nonprofessional do-it-yourself (DIY) drivers do not follow proper procedures (13, 31). In addition, monthly highway motor vehicle crashes in the United States increase from the seasonal low point in January and February, peak in July and August, and then gradually decrease in the later months of the year (32). Hence accidents represent an additional mechanism leading to slightly enhanced release of HFC-134a in summer compared with HCFC-22.

Conclusions

We used atmospheric observations from the NOAA and AGAGE networks and the ACTM model to derive global annual emission budgets for two major refrigerant gases, HCFC-22 and HFC-134a. Seasonal variations of these emissions were obtained by conducting atmospheric inversions over the 3-y HIPPO observations and validated by comparison with data from the surface networks. We find summertime emissions of both species approximately two to three times the wintertime emissions. The emission seasonality implied from HIPPO data leads to a much more accurate model simulation of the seasonally varying atmospheric concentrations of these chemicals observed in the remote atmosphere. The global emissions of HCFC-22 and HFC-134a have increased substantially over the past two decades. Because both gases are potent greenhouse gases (GHGs), there is a clear need to better locate and quantify specific emission sources and to understand the factors promoting release to the atmosphere. Our results showing significant emission seasonality suggest there may be a great potential to reduce these refrigerant gas emissions, if the design and engineering of these refrigeration systems are improved (e.g., better temperature/vibration-resistant system sealing and new system design of more compact/efficient components) (33) and if system service regulations are reinforced.

ACKNOWLEDGMENTS. We thank the Hlaper-Pole-to-Pole Observation (HIPPO), National Oceanic and Atmospheric Administration (NOAA), and Advanced Global Atmospheric Gases Experiment (AGAGE) team for measurements, especially C. Siso, P. Lang, C. Sweeney, B. Hall, and Ed Dlugokencky. We thank J. Mühle [Scripps Institution of Oceanography (SIO)], S. O’Doherty, and D. Young (University of Bristol) and P. Krummel, P. Fraser, and P. Steele [Commonwealth Scientific and Industrial Research Organization (CSIRO)] and their colleagues for access to AGAGE data. This work is supported by the following grants to Harvard University: National Science Foundation (NSF) Grant ATM-0628575 and National Aeronautics and Space Administration (NASA) Grants NNX13AH36G, NNX09AJ94G, and NNX12AI83G. It is also supported in part by NOAA’s Climate Program Office and its Atmospheric Chemistry, Carbon Cycle, and Climate Program. Support to the University of Miami comes from NSF Grant ATM-0723967. P.K.P. is supported by the Japan Society for the Promotion of Science Kakenhi Kiban-A project. AGAGE stations used in this paper are supported principally by NASA Upper Atmosphere Research Program grants to Massachusetts Institute of Technology (Mace Head, Barbados, and Cape Grim) and SIO (Trinidad Head, Samoa, Calibration), by Department of Energy & Climate Change (DECC, UK) (Mace Head) and NOAA (Barbados) grants to the University of Bristol, and by CSIRO and the Bureau of Meteorology (Australia) (Cape Grim).

1. Molina MJ, Rowland FS (1974) Stratospheric sink for chlorofluoromethanes – chlorine atom-catalysed destruction of ozone. *Nature* 249:810–812.
2. Myhre G, et al. (2013) Chapter 8: Anthropogenic and natural radiative forcing. *Climate Change 2013: The Physical Science Basis. Contribution of Working Group I to the*

5. *Fifth Assessment Report of the Intergovernmental Panel on Climate Change*, eds Stocker TF, et al. (Cambridge Univ Press, Cambridge, UK), pp 731–732, Table 8.A.1.
3. Velders GJM, et al. (2012) Climate change. Preserving Montreal Protocol climate benefits by limiting HFCs. *Science* 335(6071):922–923.

4. Rigby M, et al. (2013) Re-evaluation of the lifetimes of the major CFCs and CH_2Cl_2 using atmospheric trends. *Atmos Chem Phys* 13:2691–2702.
5. Midgley PM, Fisher DA (1993) The production and release to the atmosphere of chlorodifluoromethane (HCFC-22). *Atmos Environ* 27A(14):2215–2223.
6. McCulloch A, Midgley PM, Ashford P (2003) Release of refrigerant gases (CFC-12, HCFC-22 and HFC-134a) to the atmosphere. *Atmos Environ* 37:889–902.
7. McCulloch A, Midgley PM, Lindley AA (2006) Recent changes in the production and global atmospheric emissions of chlorodifluoromethane (HCFC-22). *Atmos Environ* 40:936–942.
8. Millet DB, et al. (2009) Halocarbon emissions from the United States and Mexico and their global warming potential. *Environ Sci Technol* 43(4):1055–1060.
9. Stohl A, et al. (2009) An analytical inversion method for determining regional and global emissions of greenhouse gases: Sensitivity studies and application to halocarbons. *Atmos Chem Phys* 9:1597–1620.
10. Stohl A, et al. (2010) Hydrochlorofluorocarbon and hydrofluorocarbon emissions in East Asia determined by inverse modeling. *Atmos Chem Phys* 10:3545–3560.
11. Saikawa E, et al. (2014) Corrigendum to “Global and regional emission estimates for HCFC-22, Atmos. Chem. Phys., 12, 10033–10050, 2012”. *Atmos Chem Phys* 14:4857–4858.
12. Siegl WO, et al. (2002) R-134a emissions from vehicles. *Environ Sci Technol* 36(4):561–566.
13. Schwarz W, Harnisch J (2003) *Establishing the Leakage Rates of Mobile Air Conditioners (B4-3040/2002/337136/MAR/C1)* (European Commission, Frankfurt, Germany).
14. Barletta B, et al. (2011) HFC-152a and HFC-134a emission estimates and characterization of CFCs, CFC replacements, and other halogenated solvents measured during the 2008 ARCTAS campaign (CARB phase) over the South Coast Air Basin of California. *Atmos Chem Phys* 11:2655–2669.
15. Barnes DH, et al. (2003) Urban/industrial pollution for the New York City–Washington, D.C., corridor, 1996–1998: 2. A study of the efficacy of the Montreal Protocol and other regulatory measures. *J Geophys Res* 108(D6):4186, 10.1029/2001JD001117.
16. Zhang YL, et al. (2010) Emission patterns and spatiotemporal variations of halocarbons in the Pearl River Delta region, southern China. *J Geophys Res* 115:D15309, 10.1029/2009JD013726.
17. Hurst DF, et al. (2006) Continuing global significance of emissions of Montreal Protocol-restricted halocarbons in the United States and Canada. *J Geophys Res* 111:D15302, 10.1029/2005JD006785.
18. Fortems-Cheiney A, et al. (2013) HCFC-22 emissions at global and regional scales between 1995 and 2010: Trends and variability. *J Geophys Res* 118:7379–7388.
19. Miller JB, et al. (2012) Linking emissions of fossil fuel CO_2 and other anthropogenic trace gases using atmospheric $^{14}\text{CO}_2$. *J Geophys Res* 117:D08302, 10.1029/2011JD017048.
20. Patra PK, et al. (2014) Observational evidence for interhemispheric hydroxyl-radical parity. *Nature* 513(7517):219–223.
21. Montzka SA, Hall BD, Elkins JW (2009) Accelerated increases observed for hydrochlorofluorocarbons since 2004 in the global atmosphere. *Geophys Res Lett* 36:L03804, 10.1029/2008GL036475.
22. Montzka SA, et al. (1996) Observations of HFC-134a in the remote troposphere. *Geophys Res Lett* 23(2):169–172.
23. Prinn RG, et al. (2000) A history of chemically and radiatively important gases in air deduced from ALE/GAGE/AGAGE. *J Geophys Res* 115:17751–17792.
24. Prinn RG, et al. (2014) The ALE / GAGE AGAGE Network, Carbon Dioxide Information Analysis Center (CDIAC), Oak Ridge National Laboratory (ORNL), US Department of Energy (DOE). Available at cdiac.ornl.gov/ndps/alegagage.html.
25. Sturrock GA, Etheridge DM, Trudinger CM, Fraser PJ, Smith AM (2002) Atmospheric histories of halocarbons from analysis of Antarctic firn air: Major Montreal Protocol species. *J Geophys Res* 107:D24, 4765, 10.1029/2002JD002548.
26. Wofsy SC, et al. (2011) HIPER Pole-to-Pole Observations (HIPPO): Fine grained, global scale measurements for determining rates for transport, surface emissions, and removal of climatologically important atmospheric gases and aerosols. *Philos Trans R Soc A* 369:2073–2086.
27. Keller CA, et al. (2012) European emissions of halogenated greenhouse gases inferred from atmospheric measurements. *Environ Sci Technol* 46(1):217–225.
28. Godwin DS, Pelt MMV, Peterson K (2014) *Modeling Emissions of High Global Warming Potential Gases* (US Environmental Protection Agency, Global Programs Division). Available at www.epa.gov/ttnchie1/conference/ei12/green/godwin.pdf. Accessed September 2, 2014.
29. Schwarz W (2001) *Emissions of Refrigerant R-134a from Mobile Air-Conditioning Systems*, Sponsorship Reference 36009006 (German Federal Environment Office, Frankfurt, Germany).
30. California Air Resources Board, Research Division (2004) *HFC-134a Emissions from Current Light- and Medium-Duty Vehicles, Technology Assessment Workshop Regarding Climate Change Emission Regulations for Light-Duty Vehicles* (California Air Resources Board, Research Division, Sacramento, CA).
31. Zhan T, Clodic D, Palandre L, Trémoulet A, Riachi Y (2013) Determining rate of refrigerant emissions from nonprofessional automotive service through a southern California field study. *Atmos Environ* 79:362–368.
32. Liu C, Chen C, Utter D (2005) *Trend and Pattern Analysis of Highway Crash Fatality by Month and Day*, Technical Report, US Department of Transportation HS809855 (National Center for Statistics and Analysis, Washington, D.C.).
33. Shah R (2008) Automotive air-conditioning systems—Historical developments, the state of technology, and future trends. *Heat Transfer Eng* 30(9):720–735.
34. Rigby M, et al. (2014) Recent and future trends in synthetic greenhouse gas radiative forcing. *Geophys Res Lett* 41(7):2623–2630.
35. Daniel JS, Velders GJM, Solomon S, McFarland M, Montzka SA (2007) Present and future sources and emissions of halocarbons: Toward new constraints. *J Geophys Res* 112(D2):D02301, 10.1029/2006JD007275.